A Nuclear Magnetic Resonance Study of the Local Conformation and Molecular Motions of Poly(N^5-(3-hydroxypropyl)-L-glutamine) in Aqueous Solution

Bruno Perly,[1a] Claude Chachaty,*[1a] and Akihiro Tsutsumi[1b]

Contribution from the Département de Physico-Chimie, Centre d'Etudes Nucléaires de Saclay, BP No. 2, 91190 Gif-sur-Yvette, France, and the Department of Polymer Science, Faculty of Sciences, Hokkaido University, Sapporo 060, Japan. *Received June 12, 1979*

Abstract: The segmental motion and local conformations of poly(N^5-(3-hydroxypropyl)-L-glutamine) (PHPG) in aqueous solution have been investigated by ^{13}C and ^1H magnetic resonance and relaxation. This polymer is a typical example of a polypeptide having a long aliphatic side chain containing a rigid core. Two widely different ^{13}C resonance frequencies, 22.7 and 63 MHz, were used to confirm the validity of the proposed motion models. ^{13}C relaxation data of C_α has been interpreted in terms of a quasi-isotropic segmental reorientation of the main chain assuming a Cole–Cole distribution of correlation times. ^{13}C and ^1H relaxation data of the side-chain methylene groups indicate a large difference in the dynamical behavior of the two parts separated by the rigid amide group. The data concerning the glutamyl methylene groups are consistent with a reorientation among three unequivalent sites, whereas the motion of the first methylene group of the hydroxypropyl fragment can be represented by a rotational diffusion about $N-C_1$. The two other methylene groups of this fragment undergo random jumps among three nearly equivalent sites. The rotamer populations assumed from the jump motions of methylene groups are consistent with those derived from proton vicinal couplings. The activation energies corresponding to the different segmental motions have been obtained from the temperature dependence of the ^1H and ^{13}C longitudinal relaxations.

I. Introduction

Synthetic homopolypeptides are the simplest models of proteins. They have been extensively used to study the parameters governing the formation and conversion of the secondary and tertiary structures in natural proteins. Thus, they are excellent models to investigate the properties of helical structures. However, since amino acid side chains are not rigid, any given activity must be related not only to the local conformation but also to the dynamical behavior of the considered group. In the last few years, much work has been devoted to the understanding of the dynamics of polymer side chains and main chains. For this purpose, nuclear magnetic relaxation methods have been found to be very convenient.[2,3] Our previous studies in this field concerned poly(L-glutamic acid).[4] We are now investigating the dynamical behavior of homopolypeptides containing side chains of various types, i.e., aliphatic, basic, and aromatic. An interesting case is that of a long linear chain with an internal rigid core. A good example of this type is provided by the poly(N^5-(hydroxyalkyl)-L-glutamines), which are expected to present several kinds of local conformations and local motions. We have thus chosen the example of poly(N^5-(3-hydroxypropyl)-L-glutamine):

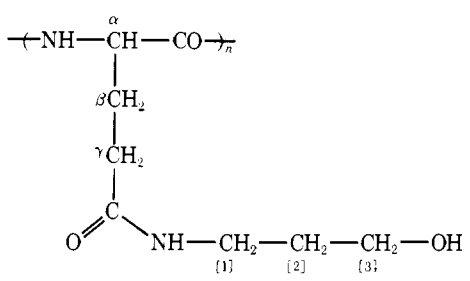

which is essentially in a coiled form in aqueous solution with a small helix content at low temperature,[5] the contribution of which is negligible under our experimental conditions.

Owing to recent advances in the field of the nuclear relaxation applied to macromolecules, several models of segmental motions can be treated by available computer programs. The selection between different models may be performed by the measurement of the longitudinal relaxation time at different Larmor frequencies. We have therefore measured the ^{13}C relaxation at 22.63 and 62.86 MHz and the proton relaxation at 250 MHz as a function of temperature.

II. Experimental Section

Materials. Poly(N^5-(3-hydroxypropyl)-L-glutamine) (PHPG) was obtained from poly(γ-benzyl L-glutamate) according to the original procedure of Lupu-Lotan et al.[6] with a few modifications. γ-Benzyl L-glutamate[7] was converted to the corresponding *N*-carboxy anhydride (NCA) by treatment with 2 equiv of 4 M phosgene in THF.[8] After two recrystallizations from ethyl acetate/petroleum ether, the NCA was polymerized as a 10% (w/v) solution in anhydrous DMF, *n*-hexylamine being used as initiator. The monomer to initiator ratio was 200. After 2 days, the poly(γ-benzyl L-glutamate) (PBLG) was isolated by precipitation in absolute methanol, washed with dry diethyl ether, and vacuum dried. Viscosity measurements in dichloroacetic acid at 25 °C according to the modified Doty equation[9a,b] indicate a molecular weight of 42 000 corresponding to an average polymerization degree of 191. PBLG (1 g) was freeze-dried from a dilute solution in dioxane and allowed to swell in 6 mL of dioxane at 75 °C for 2 h. To the stirred viscous solution, 10 mL of 3-aminopropanol was added dropwise to precipitate the polymer as a fine suspension. The mixture was flushed with dry nitrogen and allowed to stay for 20 h at 75 °C, at which time a clear solution was obtained. PHPG was isolated by precipitation in dry acetone, washed with ether, and dried. Purification was achieved by dialysis against distilled water for 5 days at 5 °C in heat-treated cellophane tubing. Final freeze-drying yielded 750 mg (90%) of PHPG as a white, expanded, fibrous material. UV absorption measurement at 257 nm indicated a complete removal of the benzyl groups. Intrinsic viscosity determination was performed in water at 28.5 ± 0.02 °C with a FICA automatic viscosimeter. The obtained value of 0.165 dL g^{-1} indicates a molecular weight of 33 400 (average polymerization degree of 180) using the viscosity law of Lupu-Lotan:[6] $\eta = 1.4 \times 10^{-5}M^{0.9}$. The comparison of this polymerization degree with that of the parent PBLG shows that very few peptide bonds were broken during aminolysis.

NMR Experiments. PHPG was twice freeze-dried from 99.8% D D_2O after treatment with a small amount of Chelex 100 chelating resin to remove possible metallic impurities. Before experiment, the calculated amount of polymer was dissolved in 99.8% D D_2O for ^{13}C measurements and in 99.95% D D_2O for ^1H. All indicated concentrations refer to monomer units. For ^{13}C experiments the concentration range was 0.6–0.7 M and for ^1H 0.05 and 0.5 M solutions were

0002-7863/80/1502-1521$01.00/0

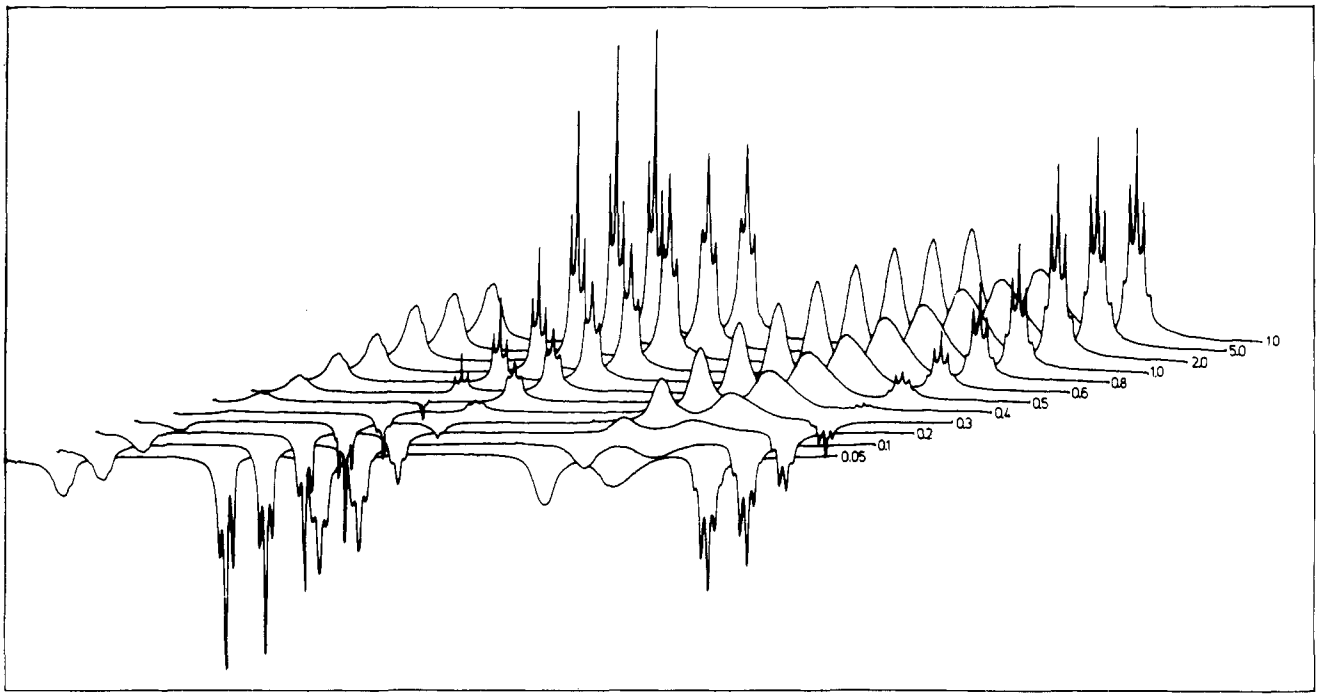

Figure 1. Stereoscopic display of an inversion recovery experiment on ^1H at 250 MHz for PHPG at 303 K. The delays between the 180 and 90° pulses are indicated. In this experiment, the delay between the pulse sequences was 8 s.

used to check the concentration dependence of the relaxation times.

Natural abundance ^{13}C spectra were obtained with a Cameca TSN 250 and a Bruker WH 90 operating at 62.86 and 22.63 MHz, respectively. All experiments were done under noise decoupling of protons. ^1H experiments were performed at 250 MHz with the Cameca TSN 250 spectrometer. In all experiments, the temperature was controlled within ±1 °C. Longitudinal spin-lattice relaxation times T_1 were obtained by the 180-τ-90 inversion recovery pulse sequence. The delay between the sequences was at least five times the largest estimated T_1. Figure 1 shows a typical stereoscopic display used for T_1 measurements. All T_1 values were obtained from the initial slope of the magnetization recovery plots with an accuracy of ±5%.

III. Theoretical Part

The calculation of ^{13}C and ^1H relaxation rates has been done under the following assumptions:

(1) The segmental motion of the macromolecular backbone is isotropic. Moreover, the experimental results suggest the existence of a distribution of the correlation time τ_c about a mean value τ_R.

(2) The motion of any methylene group of the side chain is coupled with the backbone motion and can be described by one of the three following models: model A, stochastic rotational diffusion; model B, random jumps between three equivalent sites; model C, reorientation by random jumping among three sites, two of which are equivalent.

1. Main Chain. The segmental motion of the main chain has been derived from the $^{13}C_\alpha$ longitudinal relaxation time T_1. The relaxation of this carbon being mainly induced by the directly attached proton, we have[10]

$$[T_1^{-1}]_{^{13}C} = \frac{1}{10}\gamma_H^2\gamma_C^2\hbar^2 r_{CH}^{-6} \times [J(\omega_H - \omega_C) + 3J(\omega_C) + 6J(\omega_C + \omega_H)] \quad (1)$$

γ_H, γ_C, ω_H, and ω_C being the magnetogyric ratios and Larmor frequencies, respectively. r_{CH} is the distance of a carbon to a directly bound proton.

In the case of an exponential autocorrelation function, the spectral density $J(\omega)$ is

$$J(\omega) = \frac{\tau_c}{1 + \omega^2\tau_c^2} \quad (2)$$

If there is a distribution of the correlation times τ_c defined by the probability function $G(\tau_c)$ it becomes

$$J(\omega) = \int_0^\infty \frac{\tau_c G(\tau_c)}{1 + \omega^2\tau_c^2}\, d\tau_c \quad (3)$$

In the present case we have used the symmetrical Cole-Cole distribution,[11] the density function of which is

$$F(S) = \frac{1}{2\pi}\frac{\sin(\gamma\pi)}{\cosh(\gamma S) + \cos(\gamma\pi)} \quad (4)$$

where $S = \ln(\tau_c/\tau_R)$, τ_R being the center value of the distribution. $0 < \gamma < 1$ is a parameter related to the width of the distribution; $\gamma = 1$ corresponds to a single correlation time. The relevant spectral density is

$$J(\omega) = \frac{1}{2\omega}\frac{\cos(1-\gamma)(\pi/2)}{\cosh(\gamma \ln \omega\tau_R) + \sin(1-\gamma)\pi/2} \quad (5)$$

2. Side Chain. We shall summarize here the main possible models which may be considered for the segmental motion of the side chain. The relevant expressions of relaxation rates may be found in ref 17-21.

The stochastic rotational diffusion model (model A) has been treated by several authors.[13-15] It is useful to obtain a semiquantitative picture of the mobility along a chain since the motion of each segment depends upon a single adjustable parameter. However, in the case of alkyl chains model A seems inconsistent with the relaxation data obtained at different Larmor frequencies.[21] Furthermore, it does not take into account the differences of potential energy between the different rotamers.

The model of reorientation by jumping among three sites is conveniently represented by the following scheme:

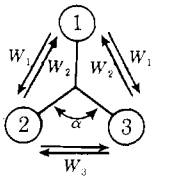

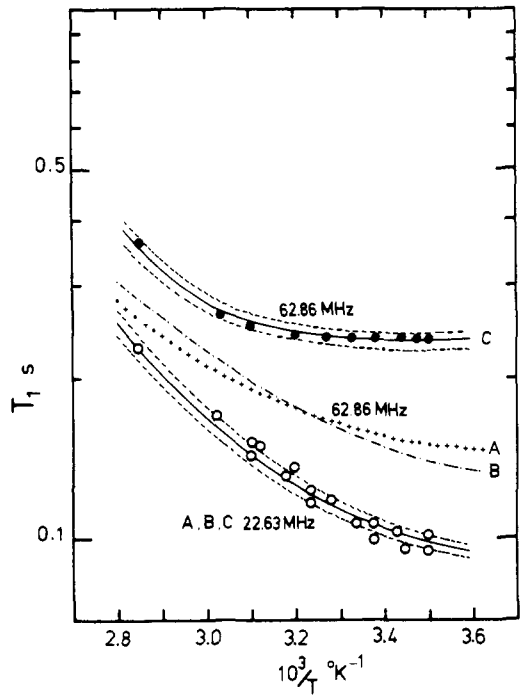

Figure 2. Selection of the most convenient model for the rotation of the $(CH_2)_\beta$ group about C_α-C_β from the ^{13}C longitudinal relaxation times at 22.63 (○) and 62.86 MHz (●). The spectrometer frequencies and the models chosen for the simulation of the temperature dependence of T_1 are indicated beside the computed $T_1 = f(1/T)$ curves. The model (C) of rotational jump among three sites with $W_1/W_2 = 0.167$ and r(C-H) = 1.09 Å yields the best agreement with the experimental T_1 at both frequencies (solid lines). The dotted lines above and below the solid lines have been computed with r(C-H) = 1.08 and 1.10 Å, respectively. The parameters for model A (rotational diffusion) and model B (jump among three equivalent sites) have been adjusted to fit the experimental T_1's at 22.63 MHz but are clearly not convenient at 62.83 MHz (+++ and -·-·-).

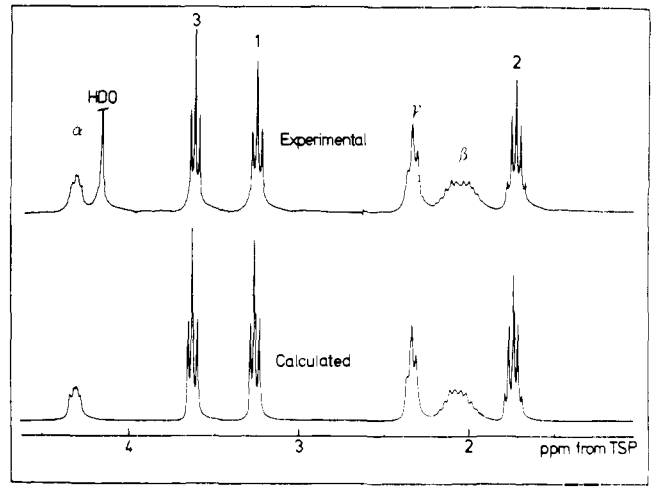

Figure 3. Observed and calculated 250-MHz ^1H NMR spectrum of PHPG at 350 K. The lower spectrum was computed from the parameters given in Tables I and II.

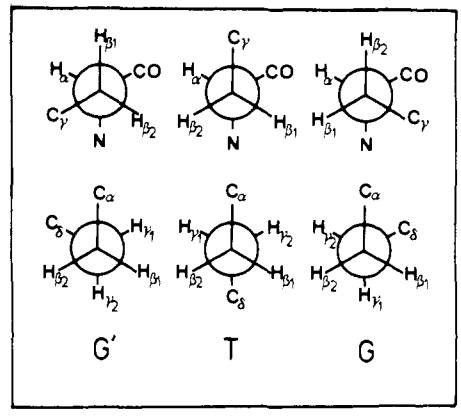

Figure 4. Definition of the different rotamers of β and γ methylene groups.

Positions 1, 2, and 3 correspond to the three possible sites among which jumps occur. W_1, W_2, and W_3 are the respective jump rates (1 → 2 and 3), (2 and 3 → 1), and (2 ⇄ 3), α being the angle between equivalent sites 2 and 3. The populations of sites 1, 2, and 3 are related to the ratio of the jump rates $v = W_1/W_2$ by

$$P_1 = \frac{1}{2v+1} \qquad P_2 = P_3 = \frac{v}{2v+1} \tag{6}$$

The original Woessner's model,[16] designated hereafter as model B, corresponds to three equivalent sites with $W_1 = W_2 = W_3$ ($v = 1$) and $\alpha = 120°$. It is often applied to the rotation of methyl groups, whereas the more general model C with $W_1 \neq W_2 \neq W_3$ is generally more convenient for methylene groups with $v \neq 1$ and $W_3 = 0$[17] or $W_3 \ll W_1, W_2$.[18-21] Lastly, the jump among two sites may be treated as a particular case of model C with either $\alpha = 0$ and v variable, according to the population of the sites 1 and 2, or $\alpha \neq 0$, $W_2/W_1 \simeq 0$, and W_3 variable.[18,21]

Most of our calculations have been performed with the standard C-H bond length of 1.09 Å (H-H = 1.78 Å). C-H distances from 1.08 to 1.10 Å may be found in the literature, the upper limit being often assumed for aliphatic residues. To these extreme values corresponds a deviation of ±6% of the computed relaxation times, with respect to those obtained from the internuclear distances given above. This deviation is of the order of experimental uncertainties as shown in Figure 2 for the example of C_β. Figure 2 illustrates also how critical is the choice of the model of internal motion for the agreement between the experimental and calculated relaxation times. For a given spectrometer frequency, the temperature dependence of the ^{13}C longitudinal relaxation may be satisfactorily simulated by adjusting the rotational diffusion constant or jump rates about each bond for any of the models A, B, or C. On the other hand, an unambiguous selection may be operated by T_1 measurements performed at very different spectrometer frequencies, e.g., 22 and 63 MHz, as in the present study. In the case of C_β, for instance, Figure 2 shows clearly that only the model C is consistent with the experimental data obtained at these frequencies. It will be shown later that this model is well supported also by proton relaxation data.

N being the number of directly bound protons for a given carbon, all our ^{13}C relaxation times will be expressed as NT_1 values. For a methylene group, the proton relaxation is mainly due to the H-H geminal interaction with $r_{HH} = 1.78$ Å. However, it is possible to take approximately into account the vicinal dipolar contribution by introducing in our calculations an effective interproton distance slightly shorter than 1.78 Å. This correction will be discussed in the next section.

IV. Results and Discussion

1. ^1H NMR Determination of the Rotational Isomerism. In the calculations of relaxation times, the ratios of jump rates between equilibrium sites depend upon their populations, which may be estimated from the $^1J_{HH}$ vicinal couplings. Figure 3 shows the 250-MHz ^1H NMR spectrum of PHPG in D_2O at 350 K. It is compared with a spectrum simulated by means of a NIC-80 computer, using the Nicolet NMRCAL program. In spite of line widths of 2.5 or 5.0 Hz, depending upon the seg-

Table I. ^1H Chemical Shifts from Internal TSP (Trimethylsilylpropionate-d_4 Sodium Salt) of PHPG in D_2O at 350 K and Line Widths Used for Spectrum Simulation at 250 MHz

	H_α	H_β	$H_{\beta'}$	H_γ	$H_{\gamma'}$	H_1	H_2	H_3
δ, ppm	4.30	2.12	2.008	2.348	2.328	3.25	1.736	3.61
$\Delta\nu_{1/2}$, Hz	5.0	5.0		5.0		2.5	2.5	2.5

Table II. ^1H Vicinal and Geminal Coupling Constants Obtained by Simulation of the ^1H 250-MHz Spectrum of PHPG at 350 K

coupling	$\alpha\beta$	$\alpha\beta'$	$\beta\beta'$	$\beta\gamma$	$\beta\gamma'$	$\beta'\gamma$	$\beta'\gamma'$	$\gamma\gamma'$	H_1H_2	H_2H_3
J, Hz	5.5	9.0	−15	7.0	7.0	7.0	7.0	−16	6.3	6.5

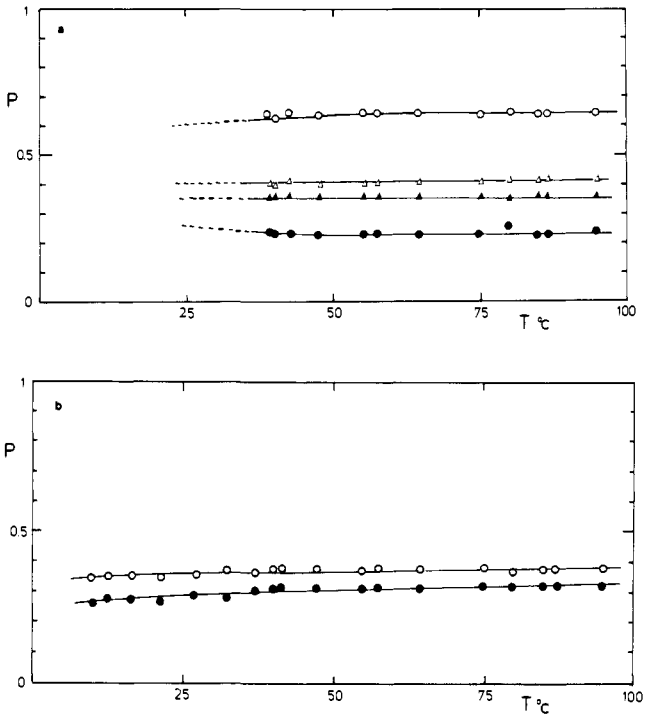

Figure 5. (a) Temperature dependence of the rotamer populations of the glutamyl group: $P_{\alpha\text{-}\beta}$ (○), $P'_{\alpha\text{-}\beta}$ (●), $P_{\beta\text{-}\gamma}$ (△), $P'_{\beta\text{-}\gamma}$ (▲). (b) Temperature dependence of the rotamer populations of the hydroxypropyl fragment: $P_{C_1\text{-}C_2}$ (○) and $P_{C_2\text{-}C_3}$ (●).

mental mobility (see section IV2), variations of ±0.5 Hz about the coupling constants and chemical shifts given in Tables I and II gave rise to significant differences between the calculated and observed spectra. The rotamer populations about each bond have been determined from the coupling constants given in Table II. We have used the Kopple modification of the Karplus relation:[22]

$$^1J_{HH} = 11.0\cos^2\theta - 1.4\cos\theta + 1.6\sin^2\theta \qquad (7)$$

θ being the $H_iC_iC_jH_j$ dihedral angle. This equation yields J_t = 12.40 and J_g = 3.25 Hz for the trans and gauche proton vicinal couplings. Figure 4 gives the definition of the G′, T, and G rotamers about the C_α–C_β and C_β–C_γ bonds. The same definition holds for the rotamers about C_1–C_2 and C_2–C_3.

The rotamer populations about C_α–C_β are given by

$$P_T = \frac{J_{\alpha\beta_1} - J_g}{J_t - J_g}$$

$$P_{G'} = \frac{J_{\alpha\beta_2} - J_g}{J_t - J_g}$$

$$P_G = 1 - P_T - P_{G'} \qquad (8)$$

Since it is not possible to assign unambiguously the β_1 and β_2 resonances there are in principle two possible solutions of eq 8:

Table III. Rotamer Populations for PHPG at 350 K

bond	P	P'	P''
C_α–C_β	0.63 = $P_{G'}$	0.24 = P_T	0.13 = P_G
C_β–C_γ	0.20	0.40	0.40
C_1–C_2	0.333	0.333	0.333
C_2–C_3	0.35	0.35	0.30

$$P_T = 0.63,\ P_G = 0.13,\ P_{G'} = 0.24$$

or

$$P_T = 0.24,\ P_G = 0.13,\ P_{G'} = 0.63$$

However, a recent work of Fischman et al.[23] concerning leucine indicates that the G′ rotamer is predominant. This conclusion was obtained from a complete set of ^1H, ^{13}C, and ^{15}N coupling constants. Moreover, in this case the ^1H couplings are very similar to ours. This behavior of the C_α–C_β bond appears to be quite general for α amino acids with a linear side chain. It is therefore reasonable to assume that in the present case the G′ rotamer is predominant.

The rotamer populations about C_β–C_γ have been calculated from the equations

$$P_T = \frac{J_{\beta_1\gamma_1} - J_g}{J_t - J_g} = \frac{J_{\beta_2\gamma_2} - J_g}{J_t - J_g}$$

$$P_G = \frac{J_{\beta_1\gamma_2} - J_g}{J_t - J_g}$$

$$P_{G'} = 1 - P_T - P_G \qquad (9)$$

The respective equilibrium positions of H_{β_1} and H_{β_2} being unknown, eq 9 gives three rotamer populations (P, P', and P'') the nature of which is undetermined (Table III). A similar situation occurs for the rotamers about C_1–C_2 and C_2–C_3, but in this case the populations are nearly equivalent (Table III). Figures 5a and 5b show that these populations have a small temperature dependence.

2. Proton and Carbon-13 Longitudinal Relaxations. The field-dependent relaxation of ^{13}C has been measured at 22 and 63 MHz. Figure 6 shows the ^{13}C NMR spectrum of PHPG at 63 MHz. No attempt was done to obtain information from the two carbonyl carbons, the relaxation time of which is very long. Their relaxation is likely not entirely dipolar, being subjected only to long-range interactions with protons. Moreover, their resonances become separated only above 50 °C.

The quasi-isotropic segmental motion of the main chain was obtained from the temperature dependence of the relaxation of C_α. Figure 7 shows the NT_1 values at 22.63 and 62.86 MHz. The solid line was calculated from eq 3 and 5 with the following parameters: activation energy ΔH = 6 kcal mol^{-1}; $\tau_0 = 4.837 \times 10^{-14}$ s; Cole-Cole distribution parameter γ = 0.70. The preexponential factor τ_0 is defined by $\tau_R = \tau_0 \exp(\Delta H/RT)$. On the same figure we have represented the effective correlation time τ_R. These results are very similar to our previous data concerning poly(L-glutamic acid)[4] and allow a satisfactory description of the quasi-isotropic segmental motion of the polymer backbone at any temperature.

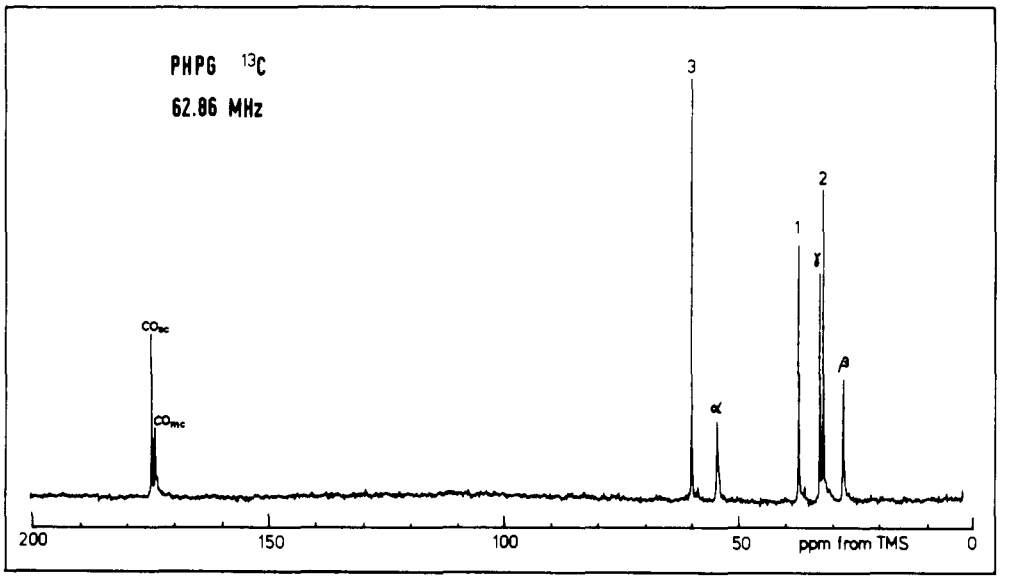

Figure 6. 62.86-MHz ^{13}C spectrum of PHPG 1 M in D_2O at 333 K. The chemical shifts were obtained from internal dioxane and are corrected relative to Me_4Si. CO_{mc} and CO_{sc} indicate respectively the main-chain and side-chain carbonyl groups.

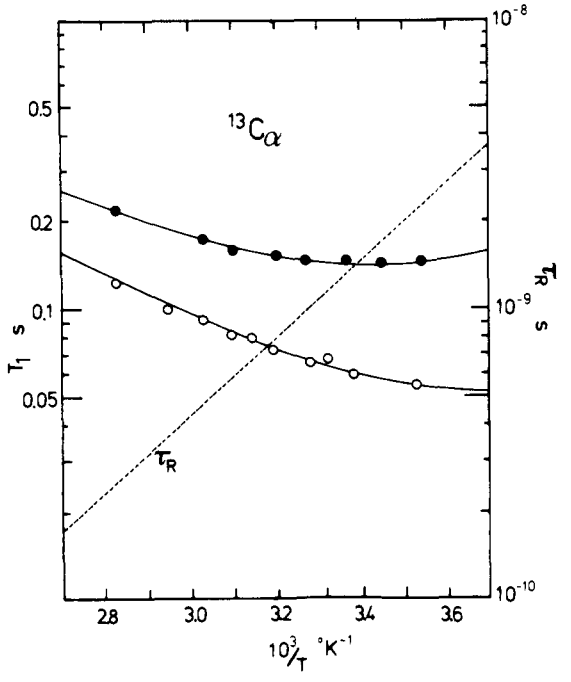

Figure 7. $^{13}C_\alpha$ relaxation times at 22.63 (○) and 62.86 MHz (●). The solid lines are calculated assuming a quasi-isotropic segmental motion of the main chain with a Cole–Cole distribution parameter $\gamma = 0.7$. The following parameters were used: $\Delta H = 6.0$ kcal mol^{-1}, $\tau_0 = 4.837 \times 10^{-14}$ s (the T_1 minimum occurs at 260 K for $\nu(^{13}C)$ 22.63 MHz). The dotted line represents the temperature dependence of the calculated effective τ_R.

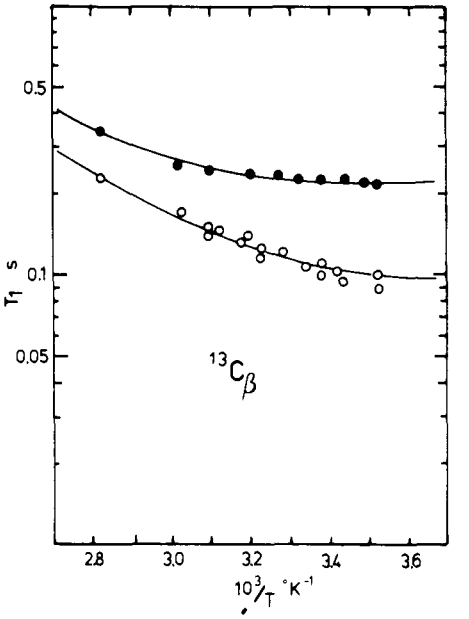

Figure 8. $^{13}C_\beta$ relaxation times at 22.63 (○) and 62.86 MHz (●). The solid lines are calculated for a three states jump model with $W_1/W_2 = 0.167$ and $\Delta H = 3.0$ kcal mol^{-1}.

The motion of $(CH_2)_\beta$ has been investigated by the relaxation of C_β. The rotamer populations derived from proton vicinal couplings being $P_{G'} = 0.63$, $P_G = 0.13$, and $P_T = 0.24$, the most convenient model is clearly the jumping between three inequivalent sites. Figure 8 shows the data obtained at two frequencies. The solid lines were calculated with the model C taking $W_1/W_2 = 0.167$. W_3, assumed to be smaller than W_1, has virtually no influence on T_1. An Arrhenius plot of W_1 yields an activation energy of 3 kcal mol^{-1}. The corresponding rotamer populations calculated from eq 6 are $P_1 = 0.75$, $P_2 = P_3 = 0.125$. These values are in reasonable agreement with those derived from the ^1H coupling constants. The important point is that only a model assuming jumps among three sites, one of them being much more populated, is consistent with the experimental data at two very different Larmor frequencies. As a verification of our model for the motion of the β-methylene group about C_α–C_β, we have calculated the relaxation time of β protons using the kinetic parameters given above. If one takes $r_{HH} = 1.78$ Å, the computed ^1H relaxation times are slightly larger than the experimental ones. The relaxation of β protons is not entirely due to geminal dipolar interactions and the contributions of α and γ protons have to be taken into account. These contributions are, however, difficult to estimate since they are likely attenuated by the rotations about C_α–C_β and C_β–C_γ; moreover, the assignment of the rotamer populations about this latter bond is ambiguous. A satisfactory agreement is, however, obtained (Figure 9) by adjusting empirically r_{HH} to 1.733 Å; i.e., the total contribution of α, γ_1, and γ_2 protons is equivalent to a proton at a distance of 2.86 Å from H_{β_1} or H_{β_2}. We have observed, moreover, that there is no concentration dependence on the relaxation of $H_{\beta_1\beta_2}$ in a range of 0.05–0.5 M in monomer units.

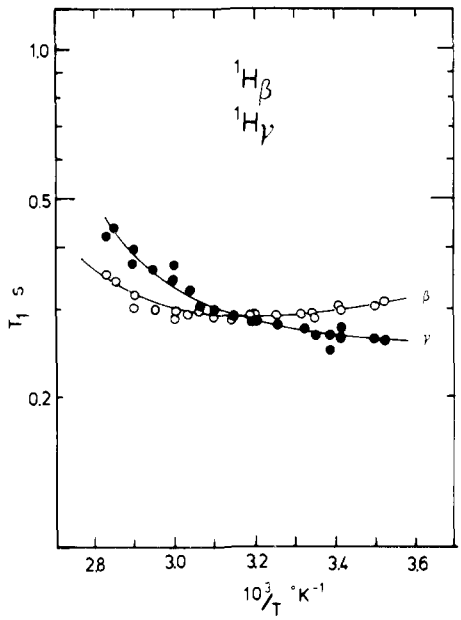

Figure 9. ^1H relaxation times of $(CH_2)_\beta$ (○) and $(CH_2)_\gamma$ (●) protons at 250 MHz. The solid lines are calculated with the kinetic parameters of Figures 8 and 10. The vicinal dipolar interactions are also taken into account (see further explanation in the text).

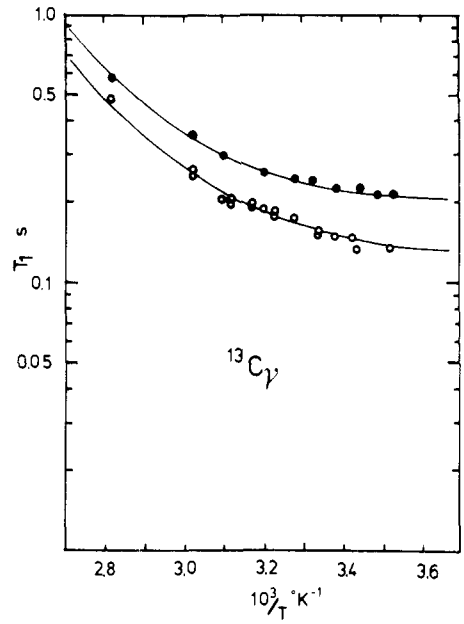

Figure 10. $^{13}C_\gamma$ relaxation times at 22.63 (○) and 62.86 MHz (●). The solid line is calculated assuming a three states jump model motion with $W_1/W_2 = 2.0$ and an activation energy $\Delta H = 5.0$ kcal mol^{-1}.

The rotamer probabilities obtained from the ^1H couplings about C_β–C_γ are $P = 0.40$, and $P' = P'' = 0.20$. It appears again that the model C must be used to describe the motion of $(CH_2)_\gamma$. The ^{13}C relaxation data at two Larmor frequencies are given in Figure 10. The solid lines are calculated with $v = 2$ and $W_3 \ll W_1$. The activation energy obtained from the Arrhenius plot of W_1 is 5 kcal mol^{-1}. The value found for v corresponds to the sites populations $P_1 = 0.2$, $P_2 = P_3 = 0.4$, which are in perfect agreement with those obtained from ^1H coupling constants. It appears therefore that about the C_β–C_γ bond two of the rotamers are equally populated, the third one being less probable. This model has been fully confirmed by ^1H relaxation at 250 MHz. Figure 9 shows the experimental results of ^1H relaxation at two polymer concentrations. The solid line was computed with the kinetic parameters used for ^{13}C simulation, taking an effective H–H distance of 1.740 Å, slightly larger than in the case of $(CH_2)_\beta$ since there are only two vicinal protons.

The rigid core formed by the peptide bond in the side chains induces a large difference in the dynamical behavior of the glutamyl and hydroxypropyl fragments. This is well evidenced in the ^1H NMR spectrum of PHPG, where the line widths of H_1, H_2, and H_3 are nearly half those of H_α, H_β, and H_γ (Table I). No information on the rotamers about the N–C_1 being available from the J coupling constant, we have tried several models for the motion of $(CH_2)_{(1)}$ about this bond and particularly the two states jump. From the ^{13}C relaxation data at two frequencies (Figure 11a) it appears that the diffusional model (model A) only is convenient. The temperature dependence of the diffusion coefficient about N–C_1 yields $\Delta H \simeq 6$ kcal mol^{-1}. Figure 11b shows the corresponding ^1H relaxation data. The solid line was calculated using the same kinetic parameters as for ^{13}C simulation and introducing a small correction of the r_{HH} distance. The value of $r_{HH} = 1.76$ Å takes into account a small contribution of the vicinal protons of $(CH_2)_{(2)}$ to the relaxation of the $(CH_2)_{(1)}$ protons. The good consistency of the diffusion model with our experimental data at three frequencies may be explained as follows. Among the three bonds existing between C_γ and C_1, rotation can occur about two of them, i.e., C_γ–CO and N–C_1. This means that there are many degrees of freedom. Even if preferential rotamers exist about C_γ–CO or N–C_1, there are always more than three possible configurations between CO and C_1. Thus, the rigid amide bond is a point of libration of the side chain and the dynamical behaviors of the glutamyl and hydroxypropyl parts are nearly independent.

For the motion inside the hydroxypropyl group, it is expected that the diffusion model is no longer valid as confirmed by ^{13}C and ^1H relaxation data which cannot be fitted simultaneously to the computed curves by use of model A.

The analysis of the ^1H NMR spectrum indicates nearly equivalent rotamer populations about C_1–C_2 so that the Woessner's model B with $W_1 = W_2 = W_3$ seems more appropriate than model C where the three equilibrium sites are inequivalent. Figure 12a shows that model B is indeed very consistent with the ^{13}C relaxation times, taking an activation energy $\Delta H = 5.9$ kcal mol^{-1} for the jump rate. The temperature dependence of $^1H_2$ relaxation time computed with the same parameters is accurately fitted to experimental data (Figure 12b) with an effective H–H distance of 1.735 Å, nearly equivalent to that found for H_β, which experiences the dipolar interaction of three vicinal protons instead of four in the present case. This may be explained by a larger reorientational freedom about C_1–C_2 and C_2–C_3 than about C_α–C_β and C_β–C_γ.

Owing to the high mobility of the $(CH_2)_{(3)}$ group, almost no frequency dependence is observed in the ^{13}C relaxation (Figure 13a). The rotational diffusion model A about C_2–C_3 being very unlikely in an aliphatic chain as seen above, we have adopted the model B for the simulation of the curves of Figure 13a because of the quasi-equivalence of the three rotamers about C_2–C_3 evidenced by the proton vicinal couplings (see Table III). In the absence of a frequency dependence of the ^{13}C relaxation, the validity of this model is confirmed by the proton relaxation (Figure 13b). The activation energy for the jump motion about C_2–C_3 is $\Delta H \simeq 6$ kcal mol^{-1}. The effective interproton distance for the simulation of Figure 12b is 1.76 Å, as for the protons of $(CH_2)_{(1)}$, which experience similar dipolar interactions with vicinal protons.

The parameters of Table IV are given as typical examples of the input data used to simulate the experimental results. An interesting observation can be made concerning the $(CH_2)_{(3)}$ methylene group. The jumping rate about C_2–C_3 is smaller than about C_1–C_2 even if the model of motion is identical. This

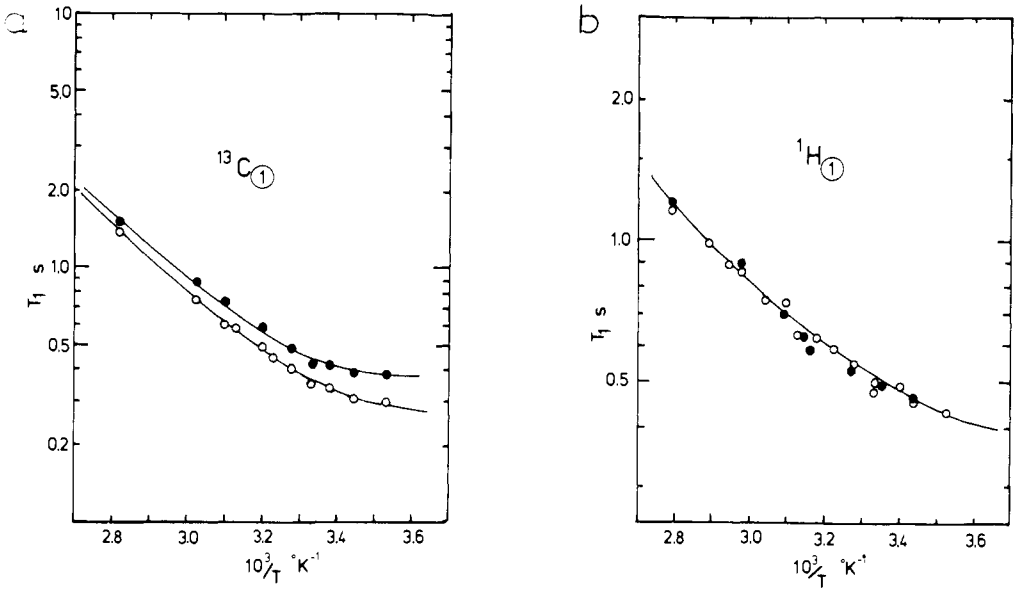

Figure 11. (a) $^{13}C_1$ relaxation times at 22.63 (○) and 62.86 MHz (●). The solid lines are calculated assuming a stochastic rotational diffusion with ΔH = 6.0 kcal mol^{-1}. (b) ^{1}H relaxation times at 250 MHz for $(CH_2)_{(1)}$ protons. Two polymer concentrations are used, i.e., 0.05 (○) and 0.5 M (●) in monomer units. The solid line is calculated using the kinetic parameters given for ^{13}C in Figure 10a and a corrected r_{HH} value of 1.76 Å.

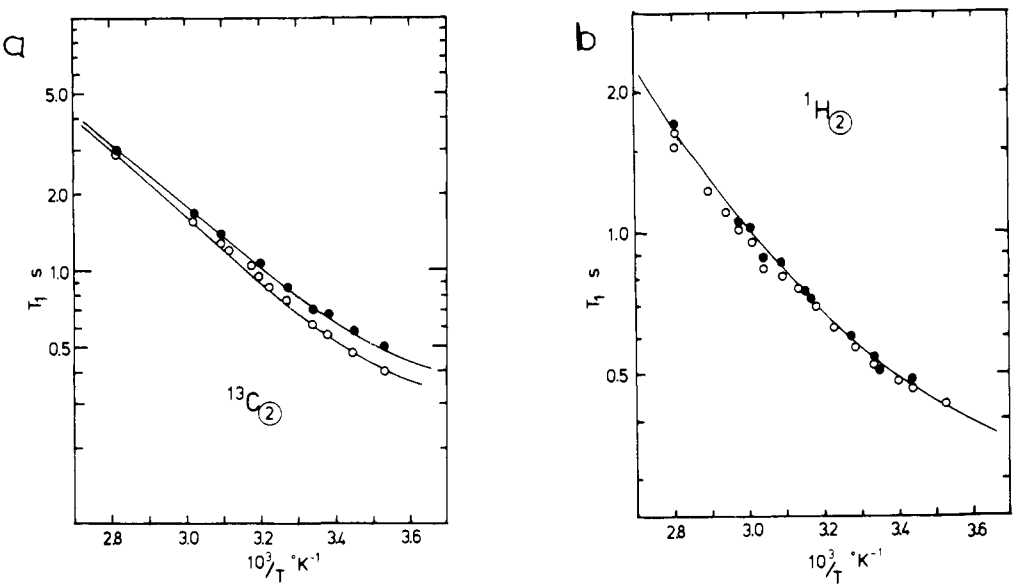

Figure 12. (a) $^{13}C_{(2)}$ relaxation times at 22.63 (○) and 62.86 MHz (●). The solid lines are calculated assuming jumps between three equivalent sites (Woessner's model) and ΔH = 5.9 kcal mol^{-1}. (b) ^{1}H relaxation data of $(CH_2)_{(2)}$ protons at 250 MHz for 0.05 (○) and 0.5 M (●) solutions. The solid line was computed from the kinetic parameters given in Figure 11a and with a corrected r_{HH} value of 1.735 Å.

Table IV. Typical Set of Kinetic Parameters Used to Simulate the ^{1}H and ^{13}C Data of PHPG[a]

nucleus	frequency, MHz	model of motion	W_1	W_2	W_3	W_1/W_2	r^*_{HH}, Å	exptl T_1, s	calcd T_1, s
$^{13}C_\beta$	22.63	C	8×10^8	4.8×10^9	0	0.167		0.13	0.130
$^{13}C_\beta$	62.86	C	8×10^8	4.8×10^9	0	0.167		0.23	0.230
$^1H_\beta$	250	C	8×10^8	4.8×10^9	0	0.167	1.733	0.3	0.296
$^{13}C_\gamma$	22.63	C	1.4×10^9	7×10^8	0	2		0.19	0.196
$^{13}C_\gamma$	62.86	C	1.4×10^9	7×10^8	0	2		0.27	0.272
$^1H_\gamma$	250	C	1.4×10^9	7×10^8	0	2	1.740	0.28	0.281
$^{13}C_1$	22.63	A	3×10^9					0.48	0.486
$^{13}C_1$	62.86	A	3×10^9					0.54	0.538
$^1H_1$	250	A	3×10^9				1.760	0.53	0.533
$^{13}C_2$	22.63	B	4.5×10^9	4.5×10^9	4.5×10^9	1		0.99	0.994
$^{13}C_2$	62.86	B	4.5×10^9	4.5×10^9	4.5×10^9	1		0.105	0.103
$^1H_2$	250	B	4.5×10^9	4.5×10^9	4.5×10^9	1	1.735	0.64	0.640
$^{13}C_3$	22.63	B	3×10^9	3×10^9	3×10^9	1		0.15	0.150
$^{13}C_3$	62.86	B	3×10^9	3×10^9	3×10^9	1		0.15	0.151
$^1H_3$	250	B	3×10^9	3×10^9	3×10^9	1	1.760	0.93	0.953

[a] These values correspond to an effective $\tau_R = 7.9 \times 10^{-10}$ s for the main chain. r^*_{HH} is the corrected distance between geminal protons. For the diffusion model A, W_1 only is meaningful and corresponds to the rotational diffusion constant.

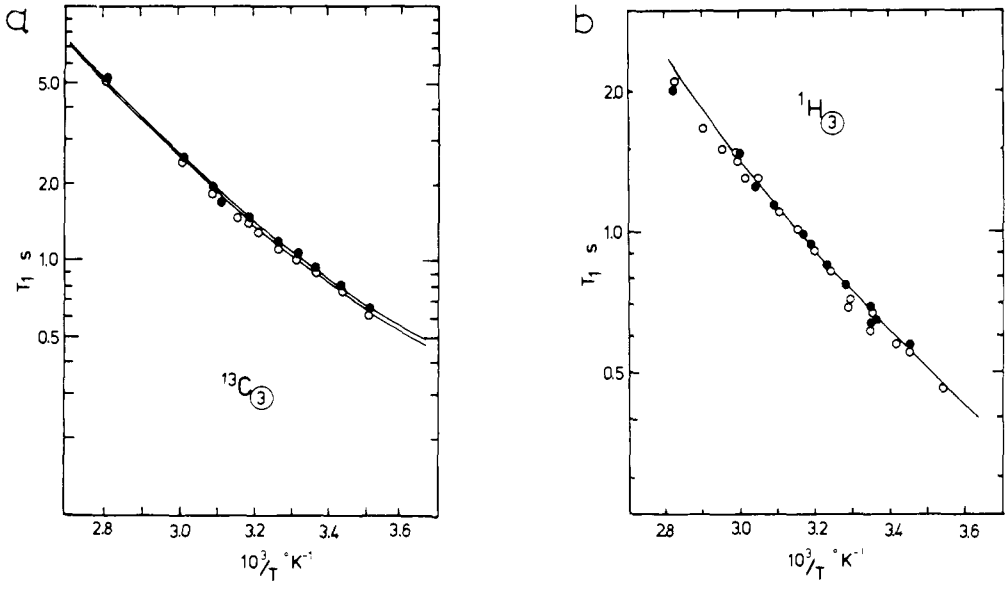

Figure 13. (a) $^{13}C_3$ relaxation data at 22.63 (○) and 62.86 MHz (●). The solid lines are calculated assuming jumps between three equivalent sites and $\Delta H = 6.0$ kcal mol^{-1}. (b) ^1H relaxation data at 250 MHz of $(CH_2)_{(3)}$ protons for 0.05 (○) and 0.5 M (●) solutions. The solid line was calculated from the kinetic parameters of Figure 12a. An effective r_{HH} distance of 1.76 Å was used to account for the vicinal dipolar contribution.

can be attributed to a solvation effect of the terminal hydroxymethyl group by water molecules which can strongly affect the intrinsic mobility about the C_2–C_3 bond relative to C_1–C_2.

V. Conclusion

We have shown in this work that the dynamical behavior of PHPG in aqueous solution is governed by fast segmental motion of the polymer backbone with effective correlation times of the order of 5×10^{-10} s at room temperature. The simple diffusion model accounts for the experimental data only in a very limited number of cases. This works confirms, moreover, the adequacy of the model of reorientation by jumps. This model was especially convenient to interpret the data of C_β and C_γ. The internal rigid amide bond induces a large difference in the dynamical behavior of the two side-chain fragments. The overall reorientation of the hydroxypropyl group about N–C_1 appears to be diffusional while the intrinsic motion of the methylene groups occurs by jumping among three sites.

This work shows, moreover, that the unambiguous choice of a motion model requires the use of several observation frequencies on different nuclei. It also appears that the results of ^{13}C and ^1H relaxation can be correlated with the rotational isomerism as determined from the ^1H coupling constants. Thus the association of conventional NMR methods and of the nuclear relaxation allows a satisfactory description of the dynamical and conformational behavior of macromolecules.

References and Notes

(1) (a) Centre d'Etudes Nucléaires de Saclay; (b) Hokkaido University.
(2) (a) A. Allerhand and P. K. Hallstone, *J. Chem. Phys.*, **56**, 3718 (1972); (b) J. R. Lyerla, Jr., T. T. Horikawa, and D. E. Johnson, *J. Am. Chem. Soc.*, **99**, 2463 (1977).
(3) D. Ghesquiere and C. Chachaty, *Macromolecules*, 11, 246 (1978).
(4) A. Tsutsumi, B. Perly, A. Forchioni, and C. Chachaty, *Macromolecules*, 11, 977 (1978).
(5) F. J. Joubert, N. Lotan, and H. A. Scheraga, *Biochemistry*, **9**, 2197 (1970).
(6) N. Lupu-Lotan, A. Yaron, A. Berger, and M. Sela, *Biopolymers*, **3**, 625 (1965).
(7) E. R. Blout and R. H. Karlson, *J. Am. Chem. Soc.*, **78**, 941 (1956).
(8) W. D. Fuller, M. S. Verlander, and M. Goodman, *Biopolymers*, **15**, 1869 (1976).
(9) (a) P. Doty, J. H. Bradbury, and A. M. Holtzer, *J. Am. Chem. Soc.*, **78**, 947 (1956); (b) N. Ho-Duc, *Can. J. Chem.*, **56**, 1569 (1978).
(10) P. Doddrell, V. Glushko, and A. Allerhand, *J. Chem. Phys.*, **56**, 3683 (1972).
(11) K. S. Cole and R. H. Cole, *J. Chem. Phys.*, **9**, 329 (1941).
(12) T. M. Connor, *Trans. Faraday Soc.*, **60**, 1574 (1964).
(13) D. E. Woessner, *J. Chem. Phys.*, **36**, 1 (1962).
(14) Y. K. Levine, P. Partington, and G. C. K. Roberts, *Mol. Phys.*, **25**, 493 (1973).
(15) G. C. Levy, D. E. Axelson, R. Schwarz, and J. Hochmann, *J. Am. Chem. Soc.*, **100**, 410 (1978).
(16) D. E. Woessner, *J. Chem. Phys.*, **42**, 1855 (1965).
(17) R. E. London and J. Avitabile, *J. Am. Chem. Soc.*, **99**, 7765 (1977).
(18) A. Tsutsumi, *Mol. Phys.*, **37**, 11 (1979).
(19) A. Tsutsumi and C. Chachaty, *Macromolecules*, **12**, 479 (1979).
(20) R. J. Wittebort and A. Szabo, *J. Chem. Phys.*, **69**, 1922 (1978).
(21) D. Ghesquiere, A. Tsutsumi, and C. Chachaty, *Macromolecules*, **12**, 775 (1979).
(22) K. D. Kopple, C. R. Wiley, and P. Tanski, *Biopolymers*, **12**, 627 (1973).
(23) A. J. Fischman, H. R. Wyssbrod, W. C. Agosta, and D. Cowburn, *J. Am. Chem. Soc.*, **100**, 54 (1978).